

---

---

# Molecular Therapy of Human Neuroblastoma Cells Using Auger Electrons of $^{111}\text{In}$ -Labeled N-*myc* Antisense Oligonucleotides

Naoyuki Watanabe<sup>1</sup>, Hiroaki Sawai<sup>2</sup>, Izumi Ogihara-Umeda<sup>3</sup>, Shuji Tanada<sup>1</sup>, E. Edmund Kim<sup>4</sup>, Yoshiharu Yonekura<sup>1</sup>, and Yasuhito Sasaki<sup>1</sup>

<sup>1</sup>Molecular Imaging Center, National Institute of Radiological Sciences, Chiba, Japan; <sup>2</sup>Department of Chemistry, Gunma University Graduate School, Gunma, Japan; <sup>3</sup>Department of Radiopharmacy, School of Pharmaceutical Sciences, Teikyo University, Kanagawa, Japan; and <sup>4</sup>Division of Diagnostic Imaging, The University of Texas M.D. Anderson Cancer Center, Houston, Texas

---

Auger electrons can create breaks in nucleic acids, giving them possible therapeutic utility. We investigated the therapeutic effect of Auger electrons emitted by  $^{111}\text{In}$ -labeled phosphorothioate antisense oligonucleotides on human neuroblastoma cells in which N-*myc* was overexpressed. **Methods:** Human SK-N-DZ neuroblastoma cells ( $5 \times 10^6$  cells) were treated with cationic reverse-phase evaporation vesicles (REVs) encapsulating  $^{111}\text{In}$ -labeled antisense (40 MBq/2 nmol of oligonucleotides/ $\mu\text{mol}$  of total phospholipids) that had an average diameter of 250 nm. Hybridization of the radiolabeled oligonucleotides with N-*myc* messenger RNA (mRNA), N-*myc* expression, and cell proliferation were investigated. The tumorigenicity of treated cells was analyzed in nude mice. Nonradiolabeled antisense,  $^{111}\text{In}$ -labeled sense, or empty cationic REVs were used as controls. **Results:**  $^{111}\text{In}$ -Labeled antisense, which hybridized with N-*myc* mRNA, was detected in cells at 12 and 24 h after the initiation of treatment. Reduced N-*myc* expression and inhibited cell proliferation were shown in the same cells at 48 h after the completion of treatment. N-*myc* expression-suppressed cells produced intraperitoneal tumors in nude mice, but the average weight of the tumors was lower than that of tumors in control mice. **Conclusion:** Auger electrons emitted from  $^{111}\text{In}$  in close proximity to their target N-*myc* mRNA may prolong the time to cell proliferation in human neuroblastoma cells due to inhibition of the translation of N-*myc*. Auger electron therapy therefore has potential as an internally delivered molecular radiotherapy targeting the mRNA of a tumor cell.

**Key Words:** Auger electrons; human neuroblastoma; N-*myc* expression; cell proliferation; molecular radiotherapy

**J Nucl Med 2006; 47:1670–1677**

---

**D**eregulation of members of the family of *myc* genes (the most common of which are *c-myc*, N-*myc*, and L-*myc*)

that encode transcription factors is found in a variety of human and animal tumors (1). Association of the N-*myc* gene with human tumor may be striking in neuroblastoma, a tumor of neural crest origin that occurs predominantly in early childhood, in which the N-*myc* gene is amplified in about 20%–25% of human neuroblastoma (2). The N-*myc* overexpression as well as the age of patients with neuroblastoma, clinical stage of disease, and regional lymph node involvement at the diagnosis are associated with poor prognosis (3–5). It has been hypothesized that deregulation of the N-*myc* gene is causative in the formation of neuroblastoma; evidence in support of this hypothesis was found in a study of transgenic mice, in which targeted expression of N-*myc* in vivo caused neuroblastoma to develop (6). Conversely, modulation of N-*myc* expression has been shown to have biologic effects—for instance, reducing the cell growth rate and inducing differentiation in human neuroblastoma cell lines. Targeted inhibitors of N-*myc* are being sought so that they can be used in the development of specific therapeutic agents for neuroblastoma with N-*myc* overexpression. To date, the biologic effects of N-*myc* modulators have been achieved by antisense oligonucleotides targeted against N-*myc* messenger RNA (mRNA) (7–9), expression vectors designed to generate N-*myc* antisense RNA (7,10), and antisense peptide nucleic acids (PNAs) against N-*myc* mRNA (PNA is an analog of DNA in which the backbone is a pseudopeptide rather than a sugar) (11). Each of these modulators has caused the translation of N-*myc* to be inhibited.

Auger electrons are a widely recognized potential candidate for use in targeted cancer therapies. DNA damage caused by Auger electrons emitted by an atom undergoing electron capture (EC) (12–16) could directly affect the oncogenes involved in the cancer's development or growth. The commercially available atoms used as Auger electron emitters are  $^{125}\text{I}$  and  $^{111}\text{In}$ . The yield of DNA strand breaks by  $^{125}\text{I}$  has been demonstrated to strongly depend on the distance between the decay site and the DNA (13), with greater damage being inflicted when the radionuclide is

---

Received Mar. 9, 2006; revision accepted Jul. 25, 2006.  
For correspondence or reprints contact: Naoyuki Watanabe, MD, PhD, Division of Human Health, International Atomic Energy Agency, Wagramer Strasse 5, P.O. Box 200, Vienna A-1400, Austria.  
E-mail: N.Watanabe@iaea.org  
COPYRIGHT © 2006 by the Society of Nuclear Medicine, Inc.

close to the gene site than when it is further away. Therefore, to estimate the extent of DNA damage in terms of strand breaks, not only the average energy of the Auger electrons but also the distance from the radionuclide to the DNA strands should be considered (17). Presumably, *N-myc* mRNA would also be broken by Auger electrons as internal radiation would be expected to cause RNA as well as DNA damage (18). Such damage similarly could result in suppressed *N-myc* expression.

In the present study, we investigated the therapeutic effect of Auger electrons on human neuroblastoma cells in which *N-myc* was overexpressed. Antisense oligonucleotides designed to bind to *N-myc* mRNA through Watson-Crick hybridization were used as a vehicle, with the assistance of cationic reverse-phase evaporation vesicles (REVs), to ensure the delivery of the Auger electrons emitted by  $^{111}\text{In}$  into the human neuroblastoma cells.

## MATERIALS AND METHODS

### Preparation of $^{111}\text{In}$ -Labeled Oligonucleotides

The sequence of the *N-myc* 15-mer phosphorothioate sense oligonucleotide was 5'-ATG CCG GGC ATG ATC-3'; it corresponded to the region of the *N-myc* mRNA beginning with the ATG start codon at position 1,650 (19). The sequence of the *N-myc* 15-mer phosphorothioate antisense oligonucleotide was 5'-GAT CAT GCC CGG CAT-3', with replacement of C-5-substituted deoxyuridine with T in the T position to conjugate isothiocyanobenzyl ethylenediaminetetraacetic acid (SCN-Bn-EDTA) (Fig. 1). The substituent at the C-5 position of T was *N*-1-acetylhexamethylenediamine (20). Oligonucleotides were assembled using an ABI 381-A DNA synthesizer (Perkin-Elmer) by means of the solid-phase phosphoramidite method, and Bn-EDTA-conjugated oligonucleotides were prepared as described by Watanabe et al. (21).

The Bn-EDTA-conjugated oligonucleotides in 100 mmol/L citrate buffer (pH 6.0) were mixed with  $^{111}\text{InCl}_3$  (Nihon Mediphsics Co., Ltd.) at a 15:1 molar ratio for 30 min at room temperature. Disodium salt EDTA ( $\text{Na}_2\text{EDTA}$ ) (Dojin Chemical

Co., Ltd.) to a final concentration of 5 mmol/L was added to the reaction solutions to chelate unbound  $^{111}\text{In}$ . The samples were subjected to 3 rounds of Sephadex G-25 (Amersham Biosciences) gel filtration in phosphate-buffered saline (PBS) without magnesium and calcium. The appropriate fractions were applied to a centrifugal concentrator (CC-105; Tomy Seiko Co., Ltd.), and the concentration of  $^{111}\text{In}$ -Bn-EDTA-conjugated oligonucleotides ( $^{111}\text{In}$ -labeled oligonucleotides) was adjusted to 410  $\mu\text{mol/L}$  in PBS. The labeling efficiency was approximately 85%. The range of specific radioactivities of  $^{111}\text{In}$ -labeled oligonucleotides was 19.7~20.3 MBq/nmol. The radioactivity was measured with a  $\gamma$ - and  $\beta$ -counting calibrator (Capintec), and the concentration of oligonucleotides was calculated from their ultraviolet absorbance at 260 nm.

The ability of the  $^{111}\text{In}$ -labeled antisense and sense and their precursors to hybridize with the synthesized 15-mer phosphodiester sense (5'-ATG CCG GGC ATG ATC-3') and antisense (5'-GAT CAT GCC CGG CAT-3') oligonucleotides was assessed by measuring the melting temperature ( $T_m$ ) with a DU-650Tm programmable spectrophotometer (Beckman Coulter Inc.). The  $T_m$  was  $54.4^\circ\text{C} \pm 0.3^\circ\text{C}$  (mean  $\pm$  SD of 3 independent experiments) of  $^{111}\text{In}$ -labeled antisense and  $54.5^\circ\text{C} \pm 0.2^\circ\text{C}$  of  $^{111}\text{In}$ -labeled sense, whereas the  $T_m$  was  $54.7^\circ\text{C} \pm 0.3^\circ\text{C}$  of phosphorothioate antisense and  $54.6^\circ\text{C} \pm 0.3^\circ\text{C}$  of phosphorothioate sense.  $^{111}\text{In}$ -Labeled oligonucleotides to a final concentration of 2.3  $\mu\text{mol/L}$  were incubated with fresh human normal serum or PBS for 96 h at  $37^\circ\text{C}$  in a humidified 5%  $\text{CO}_2/95\%$  air atmosphere, and the stability was assessed by means of reverse-phase high-performance liquid chromatography (HPLC). As free  $^{111}\text{In}$  from  $^{111}\text{In}$ -labeled antisense and sense,  $2.2\% \pm 0.2\%$  and  $2.1\% \pm 0.2\%$  of the total radioactivity, respectively, was found in serum and  $1.2\% \pm 0.2\%$  and  $1.3\% \pm 0.2\%$ , respectively, was found in PBS. The half-lives ( $t_{1/2}$ ) of  $^{111}\text{In}$ -labeled antisense and sense were  $12.2 \pm 0.3$  h and  $12.1 \pm 0.2$  h in serum, respectively.

### Preparation of Cationic REVs Encapsulating $^{111}\text{In}$ -Labeled Oligonucleotides

*N*-( $\alpha$ -Trimethylammoniumacetyl)didodecyl-D-glutamate chloride (Sogo Pharmaceutical Co., Ltd.), dilauroyl phosphatidylcholine (Sigma Chemical Co.), *L*- $\alpha$ -diarachidoyl phosphatidylcholine

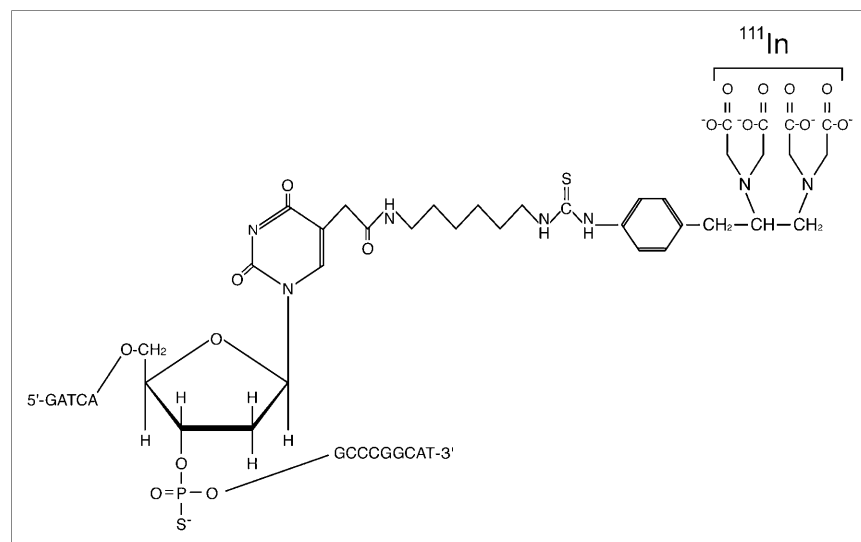


**FIGURE 1.** Structure of  $^{111}\text{In}$ -Bn-EDTA-phosphorothioate antisense oligonucleotides.

(Avanti Polar-Lipids, Inc.), and dioleoyl phosphatidylethanolamine (Avanti Polar-Lipids) in a molar ratio of 1:1:1:2 were dissolved in chloroform. Positively charged REVs were prepared according to the method described by Szoka and Papahadjopoulos (22). The lipid mixture was added to a 5-mL round-bottom flask with a long extension neck, and the solvent was removed under reduced pressure by a rotary evaporator. The system was then purged with nitrogen, and lipids were redissolved in isopropyl ether and ethanol at a volume ratio of 9:1 to obtain a final lipid concentration of approximately 10 mmol/L.  $^{111}\text{In}$ -Labeled oligonucleotides in PBS (3.6  $\mu\text{mol/L}$ ) were added at a volume ratio of 0.25 to the organic phase at this point, and the system was kept continuously under nitrogen. The resulting 2-phase system was sonicated intermittently and briefly (10–15 s) in a bath-type sonicator until the mixture became a 1-phase dispersion. The mixture was then placed on the rotary evaporator, and the solvents were removed under reduced pressure (generated by a water aspirator) at 25°C, with rotation at approximately 200 rpm.

The REV preparation was extruded 10 times through 2 stacked Nucleopore polycarbonate filters (0.2  $\mu\text{m}$ ) (Whatman Inc.) in a 10-mL capacity thermobarrel extrusion (Lipex Biomembranes).

The REV preparation was then mixed with 30% (w/v) Ficoll in PBS and transferred to a sterile cellulose nitrate centrifuge tube. Ten percent (w/v) Ficoll and PBS (in a 3:1 volume ratio) were gently layered consecutively onto the sample, and the step gradient was centrifuged at 100,000g for 30 min (Optima XL-80K centrifuge and SW55Ti rotor; Beckman Coulter Inc.) to separate cationic REVs encapsulating  $^{111}\text{In}$ -labeled oligonucleotides from unencapsulated radiolabeled oligonucleotides. Cationic REVs encapsulating  $^{111}\text{In}$ -labeled oligonucleotides with 39.4–40.6 MBq/ $\mu\text{mol}$  of total phospholipid were obtained in PBS.

The average diameters of the cationic REVs encapsulating  $^{111}\text{In}$ -labeled antisense and sense were measured as  $253.8 \pm 10.5$  nm and  $247.1 \pm 11.4$  nm, respectively, by light scattering spectrophotometry (DLS-700 spectrophotometer; Otsuka Electronics Co., Ltd.) (Fig. 2). Cationic REVs encapsulating  $^{111}\text{In}$ -labeled oligonucleotides to a final concentration of 1.14  $\mu\text{mol/L}$  of total phospholipid were incubated with fresh human normal serum or PBS for up to 24 h at 37°C, and the stability was assessed by means of a Sepharose CL-4B column (250 mm  $\times$  8 mm; Pharmacia). The cationic REVs retained  $90.0\% \pm 0.5\%$  and  $90.4\% \pm 0.5\%$  of the encapsulated  $^{111}\text{In}$ -labeled antisense and sense in serum, respectively, over 24 h and  $96.9\% \pm 0.2\%$  and  $96.6\% \pm 0.2\%$  in PBS, respectively.

#### Detection of $^{111}\text{In}$ -Labeled Oligonucleotides Hybridized with N-myc mRNA of Neuroblastoma Cells

A human neuroblastoma cell line (SK-N-DZ) was obtained from the American Type Culture Collection and maintained at 37°C in a humidified 5%  $\text{CO}_2$ /95% air atmosphere in Dulbecco's modified Eagle medium (DMEM) supplemented with 4.5 mg/L glucose, 0.1 mmol/L nonessential amino acids, and 10% fetal calf serum inactivated for 30 min at 65°C. When the SK-N-DZ cells reached logarithmic-phase growth, they were seeded in 145-mm dishes at a density of  $5 \times 10^6$  cells per dish and maintained in supplemented DMEM at 37°C in a 5%  $\text{CO}_2$  atmosphere for 24 h. Cationic REVs encapsulating  $^{111}\text{In}$ -labeled oligonucleotides (1  $\mu\text{mol}$  of total phospholipid) were added to the dishes and incubated at 37°C in a 5%  $\text{CO}_2$  atmosphere for 20 h. After REVs were then removed by washing in PBS containing 0.25% (w/v) trypsin/0.53 mmol/L EDTA, the cells were maintained in fresh

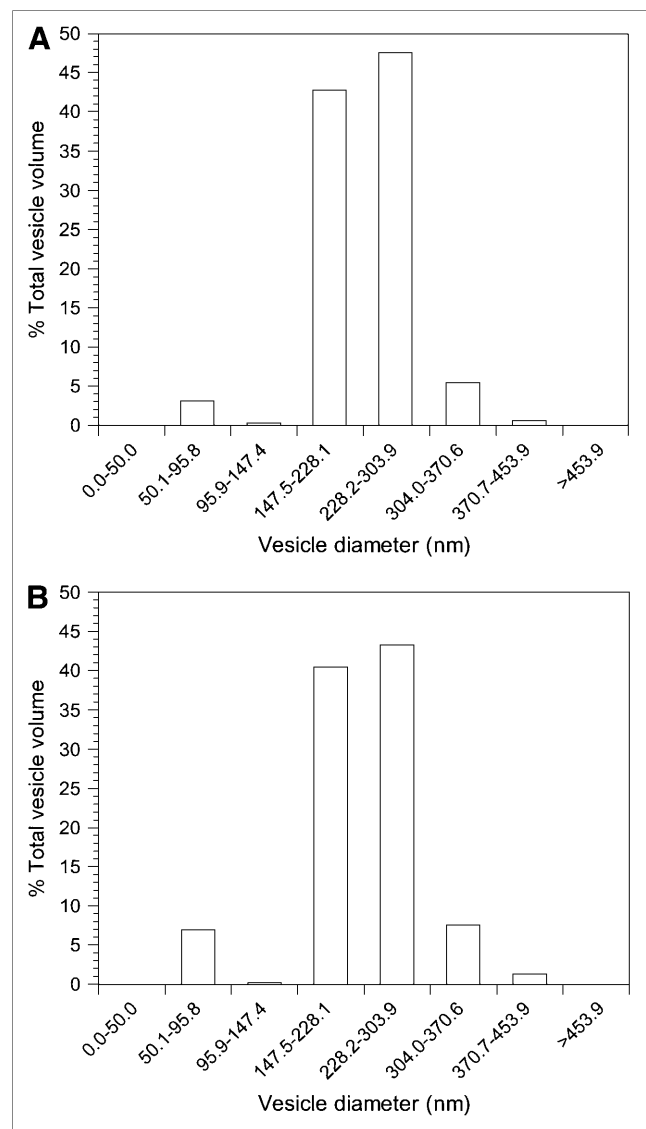


**FIGURE 2.** Size distribution of cationic REVs encapsulating  $^{111}\text{In}$ -labeled antisense (A) and  $^{111}\text{In}$ -labeled sense (B) determined by light-scattering spectrophotometer.

supplemented DMEM at 37°C in a 5%  $\text{CO}_2$  atmosphere for a further 28 h.

At 0, 12, 24, and 48 h after their exposure to cationic REVs encapsulating  $^{111}\text{In}$ -labeled oligonucleotides, cell samples were washed with 0.25% (w/v) trypsin/0.53 mmol/L EDTA in PBS and all cells in a dish were collected in a tube. The level of radioactivity was determined using a  $\gamma$ -counter (Aloka). Total RNA, including mRNA hybridized with radiolabeled oligonucleotides, was then extracted from the cells using the acid guanidinium thiocyanate/phenol/chloroform method (23). The nucleic acids were incubated in S1 nuclease buffer (280 mmol/L NaCl, 30 mmol/L sodium acetate [pH 4.4], and 4.5 mmol/L zinc acetate) with 20  $\mu\text{g/mL}$  sonicated salmon sperm DNA, containing 200 U of S1 nuclease (Takara Bio Inc.) at 37°C for 30 min. The digestion was terminated by adding 2.5 mol/L ammonium acetate and 50 mmol/L EDTA, and the sample was then fractionated by alkaline agarose gel electrophoresis (5.0% NuSieve GTG gel [FMC BioProducts], 50 mmol/L NaOH, and 1 mmol/L EDTA).

Intact  $^{111}\text{In}$ -labeled antisense and sense were also loaded as controls.  $^{111}\text{In}$ -Oligonucleotides were transferred in alkaline transfer buffer (0.4N NaOH and 1 mol/L NaCl) to a Hybond-N+ nylon membrane (Amersham) by means of the capillary transfer method. The membrane was reacted with  $^{32}\text{P}$ -labeled phosphodiester sense oligonucleotides ( $2 \times 10^6$  cpm/mL) in hybridization buffer (prehybridization buffer and 50% dextran sulfate in a 5:1 ratio) at  $42^\circ\text{C}$  for 12 h. Phosphodiester sense (5'-ATG CCG GGC ATG ATC-3') and antisense (5'-GAT CAT GCC CGG CAT-3') oligonucleotides were assembled by the synthesizer, and 5'-end labeling with [ $\gamma$ - $^{32}\text{P}$ ]ATP (111 TBq/mmol; Perkin-Elmer Life & Analytic Sciences, Inc.) was conducted with T4 polynucleotide kinase (Takara Bio Inc.). The radioactivity on the membrane was detected and quantified using an imaging phosphor plate system (BAS-1800II; Fuji Fikm Co., Ltd.) after sufficient decay of the radioindium activity of the samples. Quantitative linearity between the dose (pmol) of  $^{111}\text{In}$ -labeled oligonucleotides and the value of photostimulated luminescence was maintained. The recovery ratio of  $^{111}\text{In}$ -labeled antisense that underwent in vitro hybridization with a 60-mer RNA probe corresponding to the region of *N-myc* mRNA beginning with the ATG start codon at position 1,650) was  $9.14\% \pm 0.16\%$ . Dose corrected by the recovery ratio was expressed as the mean  $\pm$  SD of 3 independent experiments.

#### Effects of $^{111}\text{In}$ -Labeled Oligonucleotides on *N-myc* Expression in Cells and Cell Proliferation

SK-N-DZ cells in logarithmic-phase growth were seeded in 145-mm dishes at a density of  $5 \times 10^6$  cells per dish and maintained in supplemented DMEM at  $37^\circ\text{C}$  in a 5%  $\text{CO}_2$  atmosphere for 24 h. Cationic REV's encapsulating  $^{111}\text{In}$ -labeled oligonucleotides (1  $\mu\text{mol}$  total phospholipid) or cationic REV's encapsulating nonradiolabeled oligonucleotides (1  $\mu\text{mol}$  total phospholipid) that had been prepared using the methods described above were added to the dishes, which then were incubated at  $37^\circ\text{C}$  in a 5%  $\text{CO}_2$  atmosphere for 20 h. After REV's were removed by washing with 0.25% (w/v) trypsin/0.53 mmol/L EDTA in PBS, the cells were maintained in fresh supplemented DMEM at  $37^\circ\text{C}$  in a 5%  $\text{CO}_2$  atmosphere. As a control, treatment with empty cationic REV's was performed.

At 24, 48, and 72 h after the completion of treatment with cationic REV's encapsulating  $^{111}\text{In}$ -labeled oligonucleotides or nonradiolabeled oligonucleotides,  $5 \times 10^6$  cells per dish were collected into a microtube on ice and lysed in ice-cold TNE buffer (10 mmol/L Tris-HCl [pH 7.8], 1% Nonidet P-40, 150 mmol/L NaCl, and 1 mmol/L EDTA) containing 10  $\mu\text{g}/\text{mL}$  protease inhibitor aprotinin and 200 nmol/L phosphatase inhibitor sodium orthovanadate. Protein concentrations were determined by dye-binding assay (Bio-Rad Laboratories). The volume of protein solution (100  $\mu\text{g}$  of total cell protein) adjusted with TNE buffer was immunoprecipitated with anti-*N-myc* mouse monoclonal antibody (clone NCM II 100; Calbiochem) to a concentration of 5  $\mu\text{mol}/\text{L}$ , and it was subjected to 10% sodium dodecyl sulfate/polyacrylamide gel electrophoresis. Proteins were transferred onto a polyvinylidene difluoride membrane for 1 h in transfer buffer (100 mmol/L Tris [pH 8.3] and 200 mmol/L glycine) with a protein-blotting semidry system (BE-300; Bio Craft). The membrane was incubated with the anti-*N-myc* monoclonal antibody, and the antibodies were detected with rabbit antimouse IgG (Fc specific) (Fluka Chemie AG) labeled with  $^{125}\text{I}$  (Amersham) by means of the chloramine-T method (24). The radioactivity was

detected using the imaging phosphor plate system. The expression rate (given as a percentage) was calculated by dividing the  $^{125}\text{I}$  activity of *N-myc* in treated cells by that of control cells and was expressed as the mean  $\pm$  SD of 3 independent experiments. Cell count and viability were determined by trypan blue exclusion at 24, 48, and 72 h after treatment. Each experiment was performed in quadruplicate: One pair of samples was tested to determine the effect of the radionuclide on *N-myc* expression and the other pair was tested for the radionuclide's effect on cell proliferation.

#### Intraperitoneal Tumorigenicity of Human Neuroblastoma Cells with Cationic REV's Encapsulating $^{111}\text{In}$ -Labeled Antisense Oligonucleotides in Nude Mice

Six-week-old female athymic nude mice ( $n = 45$ ) with a BALB/c/*nu/nu* background (Clea Japan, Inc.) were used as an animal model for neuroblastoma in which to test the effects of  $^{111}\text{In}$ -labeled oligonucleotides. This animal study was performed in compliance with the institutional guidelines and rules governing animal care and use.

Each mouse was injected intraperitoneally with 500  $\mu\text{L}$  of 2,6,10,14-tetramethyl pentadecane (Pristan; Aldrich Chemical Co.) and was inoculated intraperitoneally with  $5 \times 10^6$  SK-N-DZ cells 1 wk later. The mice were divided equally into 3 groups, and then the cells treated with cationic REV's encapsulating  $^{111}\text{In}$ -labeled antisense and nonradiolabeled antisense were inoculated intraperitoneally into the first 2 groups, respectively, whereas the cells treated with empty cationic REV's formed the third group as a control.

Seven, 14, and 21 d after inoculation, 5 mice in each group were killed while under general anesthesia with diethylether, and tumors on the peritoneum were collected and weighed. Data obtained for each group at each time point were expressed as the mean  $\pm$  SD for 5 mice.

#### Data Analysis

Statistical comparisons were made using the Student *t* test, and differences between groups were considered statistically significant when the *P* value was  $<0.01$ .

## RESULTS

#### Detection of $^{111}\text{In}$ -Labeled Oligonucleotides Hybridized with *N-myc* RNA in Human Neuroblastoma Cells

$^{111}\text{In}$ -Labeled antisense was detectable at 12 and 24 h after the initiation of treatment (Fig. 3). For  $^{111}\text{In}$ -labeled antisense, the levels of hybridization with *N-myc* mRNA in the tumor cells were  $135.7 \pm 6.6$  pmol at 12 h and  $142.2 \pm 8.5$  pmol at 24 h;  $^{111}\text{In}$ -labeled sense was undetectable at all time points (Fig. 3).

#### Effects of $^{111}\text{In}$ -Labeled Oligonucleotides on *N-myc* Expression in Human Neuroblastoma Cells and Cell Proliferation

As shown in Figure 4, *N-myc* expression was suppressed in human neuroblastoma cells at 48 h after treatment with cationic REV's encapsulating  $^{111}\text{In}$ -labeled antisense, but it gradually recovered. However, no change in *N-myc* expression was demonstrated in the cells treated with cationic REV's encapsulating nonradiolabeled antisense at 72 h after treatment. In addition, no difference in *N-myc* expression

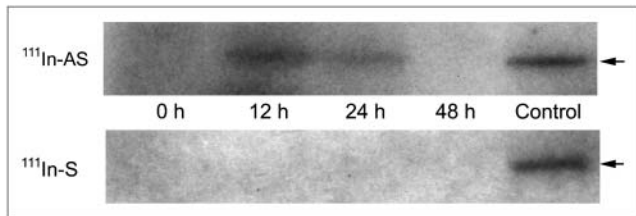


**FIGURE 3.** Detection of  $^{111}\text{In}$ -labeled oligonucleotides hybridized with *N-myc* mRNA in human neuroblastoma cells.  $^{111}\text{In}$ -Labeled antisense ( $^{111}\text{In}$ -AS) hybridized with *N-myc* mRNA at 12 and 24 h after they were exposed to cells by means of transport in cationic REV's;  $^{111}\text{In}$ -labeled sense ( $^{111}\text{In}$ -S) did not hybridize with *N-myc* mRNA. Arrow indicates radiolabeled oligonucleotides.

was noted between the cells treated with cationic REV's encapsulating nonradiolabeled antisense and the control cells (data not shown). Furthermore, no significant difference in *N-myc* expression was demonstrated between the cells treated with cationic REV's encapsulating  $^{111}\text{In}$ -labeled sense and those exposed to nonradiolabeled antisense (Fig. 5).

Proliferation of the cells treated with cationic REV's encapsulating  $^{111}\text{In}$ -labeled antisense was reduced at 48 h after treatment (Fig. 6). No difference in cell proliferation was observed between the cells treated with cationic REV's encapsulating nonradiolabeled antisense and the control cells (data not shown). The viability of the treated cells remained at >96% at 72 h after treatment.

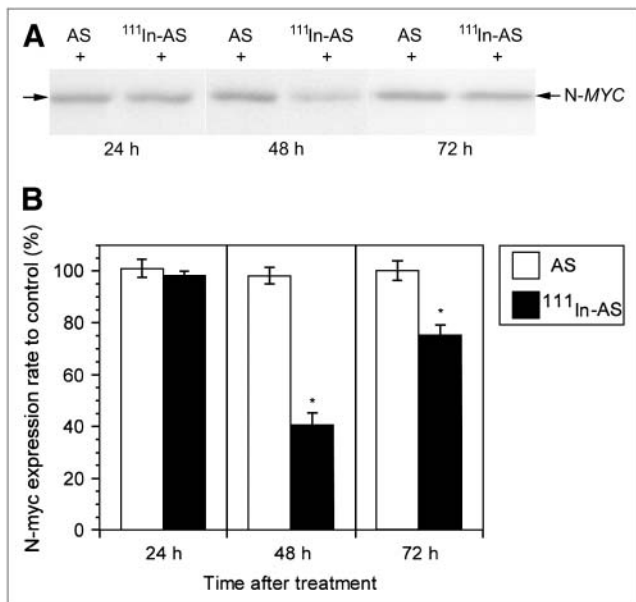


**FIGURE 4.** *N-myc* expression (*N-MYC*) in human neuroblastoma cells treated with cationic REV's encapsulating  $^{111}\text{In}$ -labeled antisense ( $^{111}\text{In}$ -AS) and nonradiolabeled antisense (AS). (A) Western blot analysis. (B) *N-myc* expression ratio of treated cells to control. Reduction in *N-myc* expression was observed in cells treated with cationic REV's encapsulating  $^{111}\text{In}$ -labeled antisense at 48 h after completion of treatment. However, nonradiolabeled antisense did not confer a significant change in *N-myc* expression in cells. \* $P < 0.01$  compared with ratio of nonradiolabeled antisense.

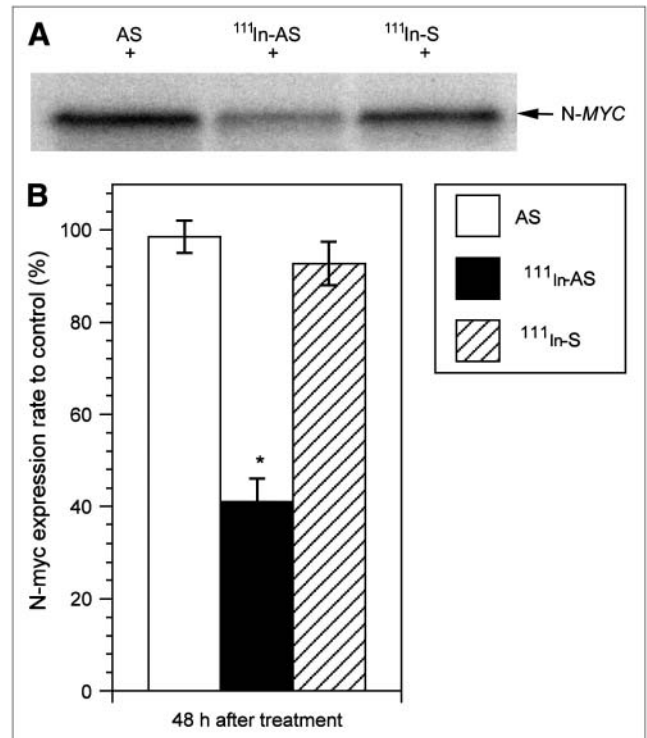


**FIGURE 5.** *N-myc* expression (*N-MYC*) in human neuroblastoma cells treated with cationic REV's encapsulating  $^{111}\text{In}$ -labeled sense ( $^{111}\text{In}$ -S). (A) Western blot analysis. (B) *N-myc* expression ratio of treated cells to control. No significant difference in *N-myc* expression was observed between these cells and those treated with cationic REV's encapsulating nonradiolabeled antisense (AS), whereas  $^{111}\text{In}$ -labeled antisense ( $^{111}\text{In}$ -AS) had shown effects at 48 h after treatment. \* $P < 0.01$  compared with ratio of nonradiolabeled antisense.

#### Intraperitoneal Tumorigenicity of Human Neuroblastoma Cells

Figure 7 shows that the cationic REV's encapsulating  $^{111}\text{In}$ -labeled antisense caused the average weight of intraperitoneal

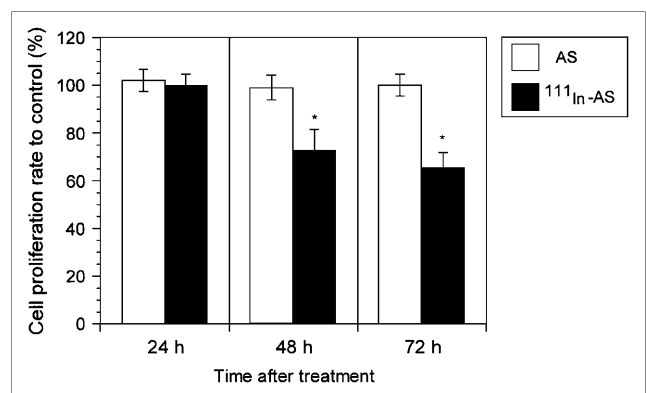


**FIGURE 6.** Cell growth in human neuroblastoma cells treated with cationic REV's encapsulating  $^{111}\text{In}$ -labeled antisense ( $^{111}\text{In}$ -AS) and nonradiolabeled antisense (AS). Cell proliferation was inhibited at 48 h after treatment of the cells with cationic REV's encapsulating radiolabeled antisense, whereas cationic REV's encapsulating nonradiolabeled antisense had no effect on cells. \* $P < 0.01$  compared with ratio of nonradiolabeled antisense.

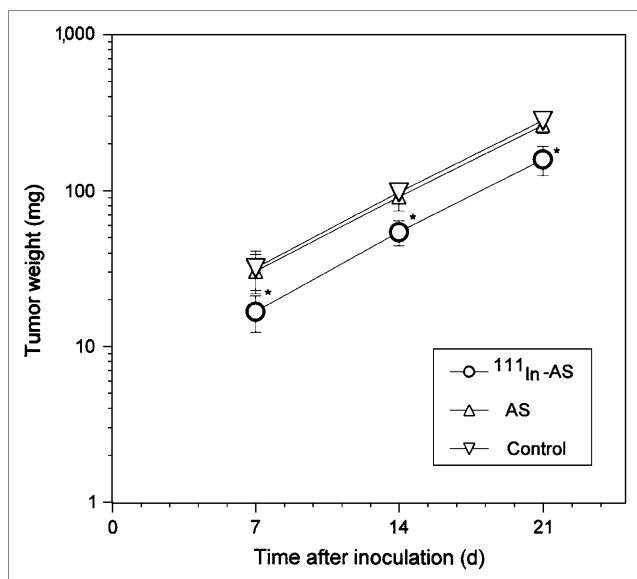


**FIGURE 7.** Tumorigenicity of human neuroblastoma cells treated with cationic REVs encapsulating  $^{111}\text{In}$ -labeled antisense ( $^{111}\text{In-AS}$ ) and nonradiolabeled antisense (AS). Cells treated with cationic REVs encapsulating radiolabeled antisense produced tumors in mice. However, average weight of tumors was lower than that of tumors produced by cells treated with cationic REVs encapsulating nonradiolabeled antisense and empty cationic REVs as a control. \* $P < 0.01$  compared with control.

tumors produced by neuroblastoma cells to decline to 48% of control or nonradiolabeled antisense treatments, although the treated cells could produce tumors in the mice. No differences in tumorigenicity were found between the cells treated with cationic REVs encapsulating nonradiolabeled antisense and empty cationic REVs as a control.

## DISCUSSION

In this study, we used Auger electrons emitted from  $^{111}\text{In}$ -labeled antisense that had been encapsulated in cationic REVs to investigate the therapeutic effects on a human neuroblastoma cell line in which *N-myc* was over-expressed.  $^{111}\text{In}$ -labeled antisense reduced *N-myc* expression in the cells and slowed cell proliferation, whereas neither nonradiolabeled antisense nor  $^{111}\text{In}$ -labeled sense did. Thus, Auger electrons that were released in close proximity to their mRNA target did cause a therapeutic effect on human neuroblastoma cells.

Because the reverse-phase evaporation method was devised for the preparation of large unilamellar vesicles (LUVs) into which DNA can be encapsulated, LUVs have been explored as a carrier for gene transfer (25–28). Modification of the positive charge of liposomes, considering that both DNA and cell surfaces are negatively charged, has enhanced gene transfer in cells in vitro (29–31). In this study, cationic REVs were prepared to (a) effectively transfer  $^{111}\text{In}$ -oligonucleotides, (b) enhance cellular uptake of  $^{111}\text{In}$ -oligonucleotides, and (c) minimize

extracellular degradation of  $^{111}\text{In}$ -oligonucleotides. Moreover, these cationic REVs may result in high tumor uptake in various tumor animal models (data not shown). Unilamellar liposome vesicles can be characterized in terms of vesicle size, as well as lipid composition, dose, and vesicle surface characteristics, such as charge and hydrophilicity (32). Small unilamellar vesicles (SUVs) are normally  $<0.1 \mu\text{m}$  in diameter, but the trapping efficiency of these materials is generally lower than that of LUVs, which range from 0.1 to 1  $\mu\text{m}$  in diameter. Reverse-phase vesicle preparation can produce LUVs that are widely heterogeneous in terms of size. This heterogeneity may dilute the potential in vivo application of LUVs because their effects could vary. To ensure reproducible effects, liposome vesicles of defined size and homogeneity should be prepared. After the LUV size was defined and homogenized by extrusion, the cationic REVs prepared in this study had a trapping volume of about 2.2  $\mu\text{L}$ , including 2.02 nmol of  $^{111}\text{In}$ -labeled oligonucleotides. The trapping efficiency was 45%, and the transfection efficiency was 13.6%.

Antisense oligonucleotides generally break targeted RNA by activation of endogenous cellular nucleases, such as ribonuclease H or the nuclease associated with the RNA interference mechanism (33). Oligonucleotides that inhibit expression of the target gene by noncatalytic mechanisms, such as modulation of splicing or arrest of translation, can also be potent and selective modulators of gene function (33). Such an antisense mechanism, however, was not expected in this study. Antisense did play a role in conveying the Auger electrons emitted by  $^{111}\text{In}$  close to the target mRNA. Although  $^{111}\text{In}$ -phosphorothioate antisense could be broken apart in cell culture medium-supplemented serum, little free  $^{111}\text{In}$  was observed in this study.

DNA strand breaks may be caused by Auger electron emitters in close proximity to DNA in vitro (12–16). One study found that during the first 30 d after treatment, most breaks caused by  $^{125}\text{I}$  were located within 10 base pairs around the decay site and that they were due to the direct action of the radioisotope rather than diffusible free radicals (13). A hydroxyl radical scavenger, dimethyl sulfoxide (DMSO), protected against damage by free  $^{125}\text{I}$  in solution, but the minimal effect on the damage was noted even in the presence of DMSO by groove-bound  $^{125}\text{I}$  (14). Another study found that decay of  $^{111}\text{In}$  produced highly localized DNA breaks over 12 d, with efficiency nearly comparable with that of  $^{125}\text{I}$  (16). A study on the effects of  $^{111}\text{In}$  decay, using diethylenetriaminepentaacetic dianhydride to restrict the intracellular kinetics of  $^{111}\text{In}$  binding to DNA, demonstrated that the average 11-fold increased effectiveness of Auger electrons of  $^{111}\text{In}$  when in proximity to DNA appears to be due mainly to the higher yield of single-strand breaks (15). Decay of the Auger electron emitters causes DNA breaks in the target gene, leading—under certain conditions—to its inactivation (34–36). We could detect  $^{111}\text{In}$ -labeled antisense that hybridized with the target *N-myc* mRNA in tumor cells at 12 and 24 h after the cells were exposed to

cationic REVs encapsulating the antisense, but this was not detected at 48 h. Reduction in *N-myc* expression, however, was observed at 48 h after treatment. These findings suggest that *N-myc* mRNA breaks were caused by Auger electrons of  $^{111}\text{In}$  in close proximity to the mRNA and that *N-myc* translation was then arrested. The effect of intracellular Auger electrons emitted by  $^{111}\text{In}$  has been demonstrated in mammalian cells in vitro (37). As little as 4.4 mBq per cell (about 4.4 MBq/L of culture) of intracellular  $^{111}\text{In}$  were able to affect the progression of cells through their first division cycle, whereas extracellular  $^{111}\text{In}$  at 1,150 MBq/mL of culture had little effect (37). About 7.5% of intracellular  $^{111}\text{In}$  was associated with DNA (37). On the other hand, in our study, the radioactivity of the  $^{111}\text{In}$ -labeled antisense integrated into the target of *N-myc* mRNA of a tumor cell at 24 h after the initiation of treatment was calculated to be about 556 mBq. Specific reduction in *N-myc* expression was caused by Auger electrons from  $^{111}\text{In}$ -labeled antisense.  $^{111}\text{In}$ -Labeled sense was incorporated into cells as much as the radiolabeled antisense, but it did not cause a significant biologic effect. These results emphasize that Auger electrons should be emitted in close proximity to their target *N-myc* mRNA.

$^{111}\text{In}$  and  $^{125}\text{I}$  have been investigated extensively as Auger electron emitters. The fact that  $^{111}\text{In}$  breaks DNA only half as effectively as  $^{125}\text{I}$  is in good agreement with the isotopes' calculated total energies and numbers of Auger electrons (16). The model of the mean absorbed dose-rate ratio of the tumor to normal tissue (TND)—a simple model that takes into account both the electron energy and the photon contribution in the evaluation of suitable radionuclides for therapy—demonstrates the importance of a low photon-to-electron energy ratio (p/e) in obtaining a high TND (17). The high abundance of photons associated with  $^{111}\text{In}$  (p/e  $\approx$  10) is predicted to reduce TND  $>5$ -fold compared with  $^{125}\text{I}$  (p/e  $\approx$  2) (17). However,  $^{111}\text{In}$  is still useful therapeutically because it is commercially and clinically available and has reliable radiochemical purity, particularly in vivo, compared with  $^{125}\text{I}$ .

Our cell proliferation study showed  $>96\%$  cell viability during the observation period, and about 27% of the cell proliferation was suppressed 48 h after treatment with the radionuclide. In the tumorigenicity portion of the study, the tumor produced by the human neuroblastoma cells treated with cationic REVs encapsulating  $^{111}\text{In}$ -labeled antisense showed about 48% weight inhibition of the control. During the observation period, however, no significant differences in tumor growth rate were detected among cells treated with radiolabeled antisense, nonradiolabeled antisense, and control (empty) REVs. Cell proliferation was suppressed after *N-myc* mRNA was damaged by Auger electrons, but it recovered with the replenishment of *N-myc* mRNA because the *N-myc* gene itself remained intact. Thus, it can be speculated that treatment with cationic REVs encapsulating  $^{111}\text{In}$ -labeled antisense may prolong the time to tumor cell proliferation but does not kill the tumor cells. The duration

of this effect may depend on the half-life of *N-myc* mRNA in the tumor cells. However, higher doses of radiolabeled antisense might cause more damage of the tumor cells. Prolongation of the time to cell proliferation might be applicable as a tumor dormancy therapy (38) by repeating the treatment. The intraperitoneal administration of cationic REVs encapsulating  $^{111}\text{In}$ -labeled antisense could be a potential approach to molecular therapy of small peritoneal metastases of neuroblastoma.

Many phosphorothioate oligodeoxynucleotides have been evaluated for their toxicologic effects in animals (39). In rodents, the most prominent toxic effects appear to be related to cytokine release induced by these agents. In monkeys, complement activation, abnormalities in clotting, and hypotensive events have been reported. However, no significant toxic effects have been observed in humans. The most probable mechanism of the observed toxic effects in laboratory animals is the binding of phosphorothioate oligodeoxynucleotides to protein (33). Different patterns of toxicity may exist between species (39). The technique used in this study, which involved use of a tiny dose of antisense labeled with  $^{111}\text{In}$ —too small to have a biologic effect on cells—and the encapsulation of antisense by cationic REVs to ensure delivery into the cells, might minimize the potential for toxicologic effects.

## CONCLUSION

Auger electrons emitted from  $^{111}\text{In}$  reduced the proliferation of human neuroblastoma cells with overexpressed *N-myc* by inhibiting *N-myc* expression. Auger electron therapy, therefore, has potential as an internal radiotherapy targeting oncogenes at the level of the mRNA.

## ACKNOWLEDGMENT

We thank Prof. Tadashi Yamamoto (Department of Oncology, Institute of Medical Science, The University of Tokyo, Tokyo, Japan) for his kind guidance in the technical aspects of molecular techniques.

## REFERENCES

1. Nesbit CE, Tersak JM, Prochownik EV. *Myc* oncogenes and human neoplastic disease. *Oncogene*. 1999;18:3004–3016.
2. Mac SM, D'Cunha CA, Farnham PJ. Direct recruitment of *N-myc* to target gene promoters. *Mol Carcinog*. 2000;29:76–86.
3. Brodeur GM, Seeger RC, Schwab M, Varmus HE, Bishop JM. Amplification of *N-myc* in untreated human neuroblastomas correlates with advanced disease stage. *Science*. 1984;224:1121–1124.
4. Evans AE, Albo V, D'Angio GJ, et al. Factors influencing survival of children with nonmetastatic neuroblastoma. *Cancer*. 1976;38:661–666.
5. Cotterill SJ, Pearson AD, Pritchard J, et al. Clinical prognostic factors in 1277 patients with neuroblastoma: results of The European Neuroblastoma Study Group 'Survey' 1982–1992. *Eur J Cancer*. 2000;36:901–908.
6. Weiss WA, Aldape K, Mohapatra G, Feuerstein BG, Bishop JM. Targeted expression of MYCN causes neuroblastoma in transgenic mice. *EMBO J*. 1997;16:2985–2995.
7. Negroni A, Scarpa S, Romeo A, Ferrari S, Modesti A, Raschella G. Decrease of proliferation rate and induction of differentiation by a MYCN antisense DNA

- oligomer in a human neuroblastoma cell line. *Cell Growth Differ.* 1991;10:511–518.
8. Larcher JC, Basseville M, Vayssiere JL, Cordeau-Lossouarn L, Croizat B, Gros F. Growth inhibition of N1E-115 mouse neuroblastoma cells by c-myc or N-myc antisense oligodeoxynucleotides causes limited differentiation but is not coupled to neurite formation. *Biochem Biophys Res Commun.* 1992;185:915–924.
  9. Rosolen A, Whitesell L, Ikegaki N, Kennett RH, Neckers LM. Antisense inhibition of single copy N-myc expression results in decreased cell growth without reduction of c-myc protein in a neuroepithelioma cell line. *Cancer Res.* 1990;50:6316–6322.
  10. Schmidt ML, Salwen HR, Manohar CF, Ikegaki N, Cohn SL. The biological effects of antisense N-myc expression in human neuroblastoma. *Cell Growth Differ.* 1994;5:171–178.
  11. Pession A, Tonelli R, Fronza R, et al. Targeted inhibition of NMYC by peptide nucleic acid in N-myc amplified human neuroblastoma cells: cell-cycle inhibition with induction of neuronal cell differentiation and apoptosis. *Int J Oncol.* 2004;24:265–272.
  12. Martin RF, Haseltine WA. Range of radiochemical damage to DNA with decay of iodine-125. *Science.* 1981;213:896–898.
  13. Panyutin IG, Neumann RD. Radioprobng of DNA: distribution of DNA breaks produced by decay of <sup>125</sup>I incorporated into a triplex-forming oligonucleotide correlates with geometry of the triplex. *Nucleic Acids Res.* 1997;25:883–887.
  14. Adelstein SJ, Kassis AI. Strand breaks in plasmid DNA following positional changes of Auger-electron-emitting radionuclides. *Acta Oncol.* 1996;35:797–801.
  15. Sahu SK, Kassis AI, Makrigiorgos GM, Baranowska-Kortylewicz J, Adelstein SJ. The effects of indium-111 decay on pBR322 DNA. *Radiat Res.* 1995;141:193–198.
  16. Karamychev VN, Panyutin IG, Kim M-K, et al. DNA cleavage by <sup>111</sup>In-labeled oligodeoxyribonucleotides. *J Nucl Med.* 2000;41:1093–1101.
  17. Bernhardt P, Forssell-Aronsson E, Jacobsson L, Skarnemark G. Low-energy electron emitters for targeted radiotherapy of small tumors. *Acta Oncol.* 2001;40:602–608.
  18. Bellacosa A, Moss EG. RNA repair: damage control. *Curr Biol.* 2003;13:R482–R484.
  19. Stanton LW, Schwab M, Bishop JM. Nucleotide sequence of the human N-myc gene. *Proc Natl Acad Sci U S A.* 1986;83:1772–1776.
  20. Sawai H, Nakamura A, Sekiguchi S, Yumoto K, Endoh M, Ozaki H. Efficient synthesis of new 5-substituted uracil nucleosides useful for linker arm incorporation. *J Chem Soc Chem Commun.* 1994:1997–1998.
  21. Watanabe N, Sawai H, Endo K, et al. Labeling of phosphorothioate antisense oligonucleotides with yttrium-90. *Nucl Med Biol.* 1999;26:239–243.
  22. Szoka F, Papahadjopoulos D. Procedure for preparation of liposomes with large internal aqueous space and high capture by reverse-phase evaporation. *Proc Natl Acad Sci U S A.* 1978;75:4194–4198.
  23. Chomczynski P, Sacchi N. Single-step method of RNA isolation by acid guanidium thiocyanate-phenol-chloroform extraction. *Anal Biochem.* 1987;162:156–159.
  24. Hunter WM, Greenwood FC. Preparation of iodine-131 labeled growth hormone of high specific activity. *Nature.* 1962;194:495–496.
  25. Mannino RJ, Allebach ES, Strohl WA. Encapsulation of high molecular weight DNA in large unilamellar phospholipid vesicles: dependence on the size of the DNA. *FEBS Lett.* 1979;101:229–232.
  26. Szelei J, Duda E. Entrapment of high-molecular-mass DNA molecules in liposomes for the genetic transformation of animal cells. *Biochem J.* 1989;259:549–553.
  27. Frezard F, Granier-Suillerot A. DNA-containing liposomes as a model for the study of cell membrane permeation by anthracycline derivatives. *Biochemistry.* 1991;30:5038–5043.
  28. Fenske DB, Cullis PR. Entrapment of small molecules and nucleic acid-based drugs in liposomes. *Methods Enzymol.* 2005;391:7–40.
  29. Bennett CF, Chiang MY, Chan H, Shoemaker JEE, Mirabelli CK. Cationic lipids enhance cellular uptake and activity of phosphorothioate antisense oligonucleotides. *Mol Pharmacol.* 1992;41:1023–1033.
  30. Yagi K, Noda H, Kurono M, Ohishi N. Efficient gene transfer with less cytotoxicity by means of cationic multilamellar liposomes. *Biochem Biophys Res Commun.* 1993;196:1042–1048.
  31. Clark PR, Stopeck AT, Ferrari M, Parker SE, Heosh EM. Studies of direct intratumoral gene transfer using cationic lipid-complexed plasmid DNA. *Cancer Gene Ther.* 2000;7:853–860.
  32. Ogihara-Umeda I, Kojima S. Increased delivery of gallium-67 to tumors using serum-stable liposomes. *J Nucl Med.* 1988;29:516–523.
  33. Dean NM, Bennett CF. Antisense oligonucleotide-based therapeutics for cancer. *Oncogene.* 2003;22:9087–9096.
  34. Hong SS, Ford EH, Alfieri AA, Bravo S. Effects of intratumoral injection of I-125 iododeoxyuridine on Ehrlich ascites carcinoma. *J Surg Oncol.* 1989;42:187–191.
  35. Yasui L, Hughes A, Desombre E. Relative biological effectiveness of accumulated <sup>125</sup>I and <sup>125</sup>I-estrogen decays in estrogen receptor expressing MCF-7 human breast cancer cells. *Radiat Res.* 2001;155:328–334.
  36. Chi KH, Wang HE, Chen FD, et al. Preclinical evaluation of locoregional delivery of radiolabeled iododeoxyuridine and thymidylate synthase inhibition in a hepatoma model. *J Nucl Med.* 2001;42:345–351.
  37. McLean JR, Blakey DH, Douglas GR, Bayley J. The Auger electron dosimetry of indium-111 in mammalian cells *in vitro*. *Radiat Res.* 1989;119:205–218.
  38. Gimbrone MA Jr, Leapman SB, Cotran RS, Folkman J. Tumor dormancy *in vivo* by prevention of neovascularization. *J Exp Med.* 1972;136:261–276.
  39. Crooke ST, Bennett CF. Progress in antisense oligonucleotide therapeutics. *Annu Rev Pharmacol Toxicol.* 1996;36:107–129.